

## DISRUPTION OF AN ALUMINA LAYER DURING SINTERING OF ALUMINIUM IN NITROGEN

Aluminium oxide layer on aluminium particles cannot be avoided. However, to make the metal-metal contacts possible, this sintering barrier has to be overcome in some way, necessarily to form sintering necks and their development. It is postulated that the disruption of alumina layer under sintering conditions may originate physically and chemically. Additionally, to sinter successfully non alloyed aluminium powder in nitrogen, the operation of both types mechanism is required. It is to be noted that metallic aluminium surface has to be available to initiate reactions between aluminium and the sintering atmosphere, i.e. mechanical disruption of alumina film precedes the chemical reactions, and only then chemically induced mechanisms may develop. Dilatometry, gravimetric and differential thermal analyses, and microstructure investigations were used to study the sintering response of aluminium at 620°C in nitrogen, which is the only sintering atmosphere producing shrinkage.

*Keywords:* aluminium, sintering, alumina layer, nitrogen atmosphere

### 1. Introduction

In view of the high oxygen affinity of aluminium, any sintering process of aluminium powder, even of the highest purity, should be considered as a sintering of a multi component system taking place in the reactive environment. From one side, oxygen is always combined with aluminium in the form of alumina layer, while from the other side, any exposed metal surface is immediately re-oxidised. It is well known that the sintering process may start when there is a direct contact between particles and mass transport by diffusion processes can create and develop sintering necks. Sintering temperature at which aluminium powder can be consolidated is far below the effective temperature of alumina sintering. Hence, a significant problem related to sintering of aluminium is to overcome the extremely stable aluminium oxide layer which is the natural sintering barrier, and to form metallic bonds, instead of alumina-alumina contacts between neighbouring particles. Since sintering of aluminium actually takes place, there has to be some mechanisms causing disruption of the aluminium oxide layer and, finally, making possible metallic Al – Al joint formation and their development. In any case, the rupture of the oxide film which exposes the underlying metal is desired to facilitate sintering of aluminium.

Although aluminium oxide layer on aluminium particles cannot be avoided, it may be disrupted under sintering conditions. Disruption of the alumina layer may originate physically and chemically and to sinter successfully “pure” aluminium, the operation of both mechanisms is required. It is to be noted that metallic aluminium surface has to be available to initiate reactions

between aluminium and the sintering atmosphere, i.e. mechanical disruption of alumina film precedes the chemical reactions, and only then chemically induced mechanisms may develop.

The mechanical rupture of the alumina layer during compaction of aluminium powder may enhance its sintering process. Nevertheless, disruption of the oxide layer alone should not be considered as a sufficient mechanism causing strong bonds to form between aluminium particles, because a part of the exposed metal surface will be immediately re-oxidised and, of course, the initial amount of the oxide will not be reduced [1-3].

Physical nature mechanisms of alumina film spalling are related to the temperature changes and comprise:

- thermal stresses,
- amorphous alumina → crystalline  $\gamma$ -Al<sub>2</sub>O<sub>3</sub> transformation,
- aluminium evaporation, and
- local melting.

In turn, the chemical type mechanisms comprise:

- self-gettering, and
- aluminium reactions with nitrogen and oxygen.

The purpose of this review paper is to demonstrate the validity of all these possible ways to overcome the natural sintering barrier which is alumina layer for aluminium sintering.

### 2. Thermal stresses

For any two layer system, thermal stresses arise due to changes in temperature when the film and substrate have different coefficients of thermal expansion (CTE). For a large difference

\* AGH UNIVERSITY OF SCIENCE AND TECHNOLOGY, AL. MICKIEWICZA 30, 30-059 KRAKÓW, POLAND.

# Corresponding author: pieczonk@agh.edu.pl

in thickness of the coating and substrate ( $h/H \ll 1$ ), which is the case for alumina layer covering aluminium powder particle of micrometer size, the film has little effect on the substrate and the substrate imposes its strains on the film. Thus, assuming that the coefficients of thermal expansion do not vary with temperature, the thermal mismatch stress  $\sigma_{th}$  in the film may be estimated from the following equation [4]:

$$\sigma_{th} = \frac{E_f (\alpha_s - \alpha_f) \Delta T}{1 - \nu_f} \quad (1)$$

Where  $E_f$ ,  $\alpha_f$ ,  $\nu_f$  are Young's modulus, thermal expansion coefficient and Poisson's ratio of the film material, respectively,  $\alpha_s$  is the thermal expansion coefficient of the substrate material, and  $\Delta T$  the temperature change.

Thermo-mechanical data collected in Table 1 were used to estimate the thermal stresses in the alumina layers. Generally, since the CTE of the aluminium substrate is higher than that of the alumina film, the tensile stresses can be expected in the film when temperature rises. Assuming the absence of residual stresses in the alumina film at room temperature, the mismatch stresses generated within the amorphous layer (i.e. up to 450°C when it transforms into crystalline  $\gamma$  – phase) may be within the range 200 – 850 MPa, while in case of  $\gamma$  – alumina the temperature change of 100°C may involve stresses between 720 and 816 MPa. Detailed calculations, to be reported later, need to take account of the size and geometry of the irregularly shaped aluminium powder particles and thickness of the alumina layer. Generated tensile stresses in the alumina are sufficiently high to induce cracking of the alumina layer covering aluminium particles and thus to expose locally the metallic surface.

TABLE 1

Thermo-mechanical properties of aluminium, alumina and aluminium nitride

Material	CTE 10 <sup>-6</sup> / K	Young's modulus, GPa	Poisson's ratio
Al solid	23.03 [5]	72.2 [5]	0.34 [5]
Amorphous alumina	10 – 20 [6]	122 [7]	0.20 [8]
$\gamma$ – Al <sub>2</sub> O <sub>3</sub>	6.5 – 8.9 [5]	387 [7]	0.24 [9]
Aluminium nitride	4.5 [35]	330 [35-37]	0.24 [35]

In spite of the significant difference in thermal conductivity of aluminium and  $\gamma$  – alumina, 237 vs. 39 W/mK [5], respectively, thermal stresses induced by this difference during heating can be neglected because of the low thickness of the alumina film and rather low heating rates (~10 K/min.).

### 3. Transformation of amorphous alumina into crystalline $\gamma$ – Al<sub>2</sub>O<sub>3</sub>

The amorphous alumina film covering aluminium powder particles transforms during heating into the more stable crystalline  $\gamma$ –Al<sub>2</sub>O<sub>3</sub> phase. Atomic rearrangements in the alumina layer are responsible for its densification, since  $\gamma$ –Al<sub>2</sub>O<sub>3</sub> has a higher

density than amorphous alumina (Table 2). The difference ranges from about 10 up to 40% because the density of the amorphous phase of alumina varies over an exceptionally large range, between 2.1 and 3.5 g/cm<sup>3</sup> [10-12], which suggests the existence of amorphous polymorphism [12,13]. Anyway, for the alumina film covering aluminium powder particles, the specific volume ratio  $\gamma$ –Al<sub>2</sub>O<sub>3</sub> / Al of ~1.2 is generally assumed [15]. In any case, due to this transformation, the formation of micro-cracks in the oxide layer is inevitable which results in exposing the underlying aluminium metal.

TABLE 2

Densities of phases expected in aluminium during its sintering in nitrogen

Material	Density, Mg/m <sup>3</sup>	Source
Amorphous Al <sub>2</sub> O <sub>3</sub>	2.10 – 3.50	[10-12]
$\gamma$ – Al <sub>2</sub> O <sub>3</sub>	3.60	[12]
Al solid at m.p.	2.70	[14]
Al liquid at m.p.	2.39	[14]
AlN	3.23 – 3.28	[34]
AlON	3.67 – 3.69	[38]

For comparison, the most stable alumina, i.e.  $\alpha$  – Al<sub>2</sub>O<sub>3</sub>, has a density of 3.98 Mg/m<sup>3</sup> [12]. Due to the transformation of amorphous alumina into the crystalline  $\gamma$  – Al<sub>2</sub>O<sub>3</sub> phase, a network of grain boundaries is formed within the oxide layer. Thus, the paths for enhanced diffusion of reactants become available. Hence, the presence of micro-cracks and grain boundaries may facilitate the direct contact between aluminium surface and nitrogen molecules and in this way the sintering process.

### 4. Aluminium evaporation

Aluminium partial pressure at 620°C is about  $5 \times 10^{-13}$  bar [16]. The direct role of aluminium evaporation, if any, in mechanical disruption of alumina layer can be marginal. However, aluminium vapour may take part in reactions with the sintering atmosphere, evolving a great amount of heat and, in this way, may influence liquid phase formation, which, in turn, may play a role in the rupture of the oxide film and thus facilitate sintering of aluminium. Furthermore, it should not be completely discounted that the extremely high exothermic reaction between aluminium vapour and atomic nitrogen may be responsible for initiation of the intense densification of aluminium compacts observed during isothermal sintering [2,3,25].

### 5. Local heating of the sintered system, resulting in higher local temperature than that of the furnace, and local melting

Researchers investigating the sintering mechanisms of aluminium and its alloys tend to agree [2,3,17-25] that successful sintering requires a liquid phase that penetrates the stable, but

spalled, aluminium oxide film covering the powder particles. For any aluminium based pre-alloyed powder or elemental powder mixture the appearance of a liquid phase during sintering results from the presence of alloying elements, like Cu, Mg, Zn, Sn, forming low melting point alloys with Al. In the case of high purity aluminium powder, however, the formation of a liquid phase below the melting point of Al requires a nitrogen atmosphere that can exothermally react with aluminium and, in this way, locally heat the material above its melting point. Thermal analysis DTA, TG, DSC and dilatometry experiments performed on aluminium powder in a high purity nitrogen atmosphere [2,3,20-25] indicate both strong exothermic reactions and densification occurring at a high rate, which is specific to liquid phase sintering.

It is well known in industrial practice that nitrogen of high purity and low dew point is a particularly well suited sintering atmosphere for aluminium. As was proved experimentally [2,3,20,24,25], the reactions of aluminium with nitrogen producing aluminium nitride AlN are responsible for the effective sintering of this metal. Of course, the reaction may be induced if there is direct contact between the metallic aluminium surface and nitrogen. As shown earlier, thermal stresses and polymorph transformation of alumina are responsible for disruption of the alumina layer. Since immediate re-oxidation of exposed aluminium tends to occur, the reaction of aluminium with nitrogen may become possible when the aluminium oxidation reaction is suppressed, which, in turn, requires extremely low oxygen partial pressure. The latter may be achieved in the interior of the sintered compact due to self-gettering, where the outer part of the compact acts as a getter [2,3,20,25]. Thus, the reduction of oxygen partial pressure below the critical level and thermal destruction of the alumina film, creating fresh aluminium surfaces within the pores, can allow nitrogen gas to react with aluminium. It may also be added that, although aluminium has a high affinity for oxygen and is preferentially oxidised over nitriding, the formation of the oxide layer is not only controlled by thermodynamics. As LECO analysis showed [2,3,24,25], significant aluminium nitriding evolved within the internal part of the compact is accompanied by a slight oxidation (Table 3). Both aluminium nitriding and oxidation are highly exothermic reactions.

TABLE 3

Oxygen and nitrogen contents within the external and internal zones of the sintered aluminium specimen [25]

Zone of the sintered compact	Oxygen content, [mass %]	Nitrogen content, [mass %]
External layers	1.64 – 4.03	0.015 – 0.354
Interior	0.49 – 1,42	0.855 – 4.290

The amount of heat generated due to the exothermic reactions may be estimated by evaluation of the DSC curve registered during isothermal sintering of aluminium in nitrogen (Fig. 1). It should be noted that both shrinkage and release of heat proceed isothermally if the furnace temperature is taken into consideration.

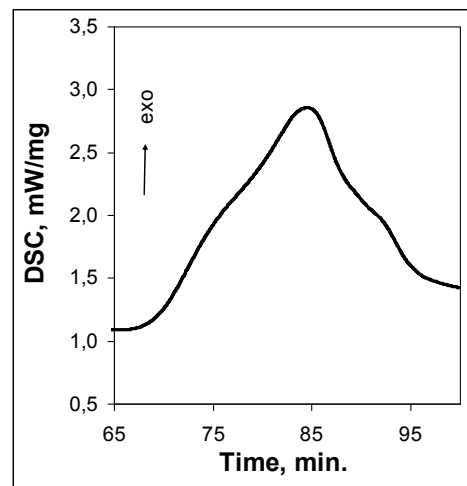


Fig. 1. Detailed DSC curve for isothermal sintering of tap density aluminium powder layer, temperature 620°C, nitrogen 5N [24]

Integrating the area below the exothermal peak gives the value of 1473 J/g. Since the specific heat of aluminium is 0.9 J/gK, about 45 J of energy is sufficient to raise the temperature of 1 g Al by 50°C. Hence, only ~3% of released energy is sufficient to increase locally the temperature within the sintered aluminium above its melting point. In spite of the width of the exothermal event, ~37 min., the melting point of aluminium may locally be exceeded. Dilatometry investigations and metallographic analysis [3,25] fully confirm this assumption. The microstructure of the internal part of the aluminium compact sintered in nitrogen is shown in Figure 2.

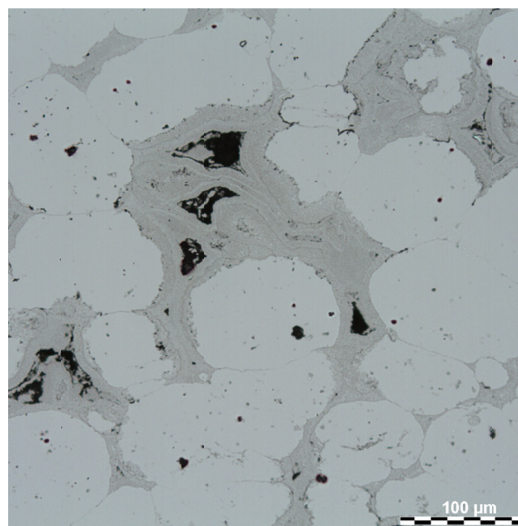


Fig. 2. Microstructure of the interior of an aluminium compact sintered in nitrogen. Isothermal sintering temperature – 620°C

It should be added that the amorphous-to-crystalline transformation in alumina is also exothermic, but, with enthalpy change only of the order of –50 J/mol, it is not expected to be a significant source of energy. There is, however, a report that documents local interfacial melting of aluminium due to the amorphous alumina transformation [26].

The melting of aluminium is accompanied by a relatively large volume increase of  $\sim 12\%$  (Table 2). Hence, the surface liquid will promote further disruption of any remaining oxide film. Furthermore, liquid aluminium may penetrate the interface aluminium/alumina and also in this way destroy the oxide film, similarly to that shown for the Al-Cu system [18]. With regard to the greater volume expansion coefficient of the melt than of solid aluminium, this melt can also affect oxide crust degradation as a result of its local expansion.

There are also other consequences of local overheating and melting. One of them is related to the increase of the partial pressure of aluminium vapour, which rises from about  $5 \times 10^{-13}$  to  $3.5 \times 10^{-12}$  bar [16] as temperature rises from  $620^\circ\text{C}$  to  $660^\circ\text{C}$ . Since the reaction of aluminium vapour with nitrogen, in particular with atomic nitrogen, is extremely exothermic, it is possible that this reaction starts the sintering reaction sequence. Additionally, there is also a report [27] that nitrogen molecule  $\text{N}_2$  dissociates readily on the surface of liquid aluminium, since the dissociation energy barrier is only  $-3$  eV. As thermodynamic calculations show, atomic nitrogen is highly reactive, not only with gaseous and liquid aluminium, but also with solid metal, which easily forms aluminium nitride. Therefore nitriding of solid aluminium may be also a further substantial source of heat.

Whereas published phase diagrams [28-32] postulate little, or no, nitrogen solution in solid aluminium, THERMOCALC indicates some solubility with accompanying decrease in the melting temperature [33]. Calculations indicate nitrogen contents of 0.09 and 0.32% in the solid and liquid phases at  $620^\circ\text{C}$ , respectively. Accordingly DTA runs were made [33] with small pieces of fully-dense pure aluminium used as a standard, and with powders and compacts, to above its melting point in pure argon and in pure nitrogen (Fig. 3). It is to be noted that melting commences in nitrogen some  $12^\circ\text{C}$  lower than in argon. The results clearly imply that the effect of nitrogen on temperature of liquid formation may be attributed to the limited solid state solubility of nitrogen in aluminium.

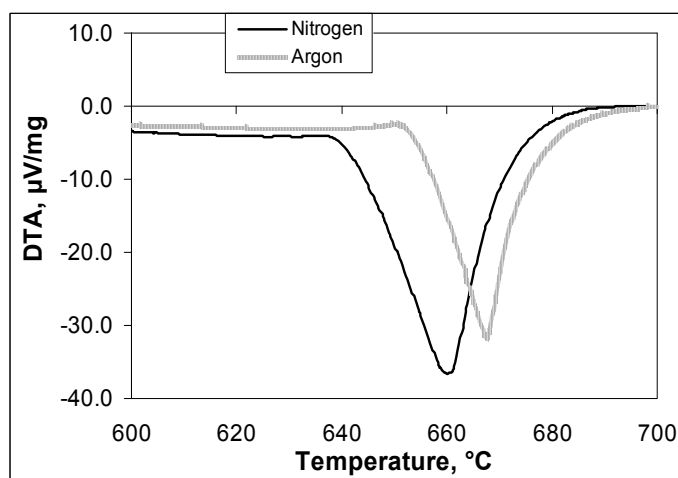


Fig. 3. DTA traces for pure fully-dense aluminium solid heated to above the recognized melting point at  $10^\circ\text{C}/\text{min}$  in atmospheres of pure argon and nitrogen, respectively. Note that melting in nitrogen commences some  $12^\circ\text{C}$  lower [33]

To conclude: the combined exothermal energy may take the local temperature to a significantly higher level than the furnace sintering temperature and hence possibly promote the breaking of the nitrogen triple bonds, thus forming atomic nitrogen and also promote melting of the aluminium.

It may also be noted that, after a liquid appears in sintered aluminium compacts, processes specific to the liquid phase sintering start to operate. It is well known that a liquid phase that wets the solid surface is beneficial for densification by the particles' rearrangement mechanism. Since this is the case for the system analysed, the occurrence of particle reorganisation causes enhanced pore shrinkage and, finally, a significant compacts' densification takes place [2,3,25].

## 6. Selfgettering

Microstructural investigations and LECO analysis of sintered aluminium compacts [2,3,25] clearly show that the reactions in the interior of the specimen differ qualitatively and quantitatively from those at and near the surface. Inhomogeneous microstructures of sintered aluminium (Figs 4 and 5) are attributed to the self-gettering phenomenon [20]. It is suggested that during sintering of aluminium in nitrogen, the outer layers of the porous compact serve as a getter for the inner section, such that oxygen partial pressure is reduced deep within the pore network. In this way the outer layer of compact becomes more oxidised and poorly sintered, while exothermal reactions of aluminium with nitrogen become possible in the interior.

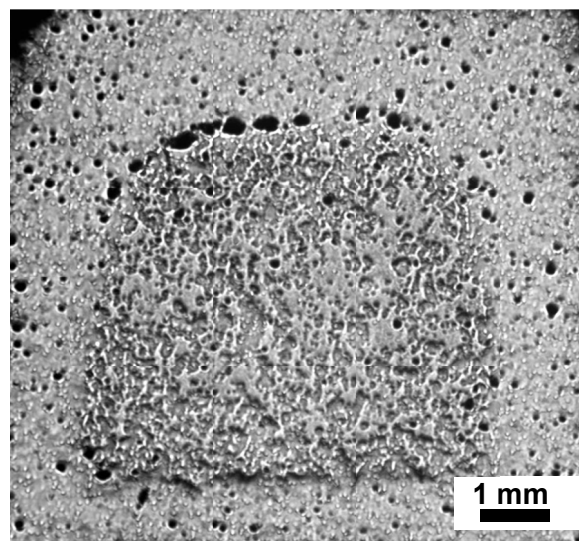


Fig. 4. Cross section of the "gradient sintered" aluminium compact seen on the macroscopic level. Specimen was made of high purity Al powder, green density – 80%, isothermal sintering temperature –  $620^\circ\text{C}$ , and time – 2h, sintering atmosphere – high purity nitrogen. Heterogeneous structure consists of easily distinguishable zones: the superficial external layers (oxidised Al) and darker interior (nitrided Al)

Microstructural observations (Fig. 5) reveal very clearly the differences between the porous sintered zone located at the

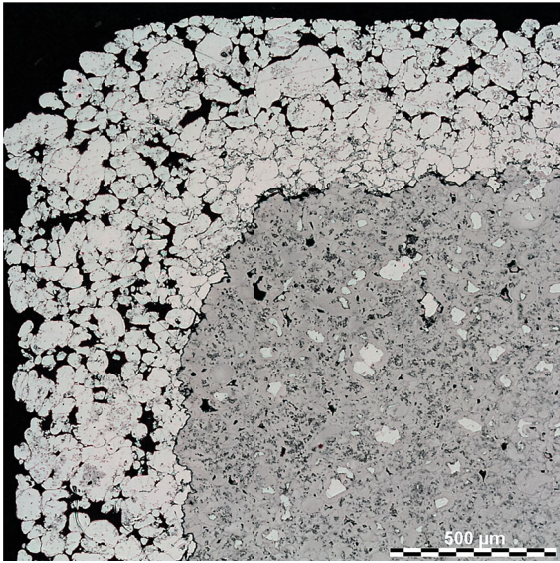


Fig. 5. Optical micrograph of the outer part of the sintered Al specimen from Figure 7.4. From the left: poorly sintered porous surface layer, well sintered intermediate dense and free of nitriding products Al layer, and highly nitrided interior

surface of the specimen and the interior of the sample, which is well sintered without residual porosity. Powder particles, roughly of the initial sizes and shapes, poorly joined or even partly separated, can be observed within the surface layer, which is evidence of limited development of sintering in this zone. Because of the weak bonding between particles, mechanical properties of this layer, such as strength and wear resistance, are considerably lower than those required and expected of well-sintered materials.

It is worthwhile noting that the getter function of aluminium becomes possible owing to the disruption of alumina layers during heating, which exposes metallic surface of aluminium to the atmosphere. The reduction of oxygen partial pressure within the connected pores of the compact may allow alumina transformation to non-stoichiometric oxy-nitrides and the formation of aluminium nitride AlN. This was confirmed by metallographic and EDX examinations [30]. The conversion of  $\gamma\text{-Al}_2\text{O}_3$  to AlN can contribute to further disruption of alumina layer, as  $\gamma\text{-Al}_2\text{O}_3$  has a higher density than AlN (Table 2), while aluminium oxynitride formation is unlikely to have any influence on dimensional changes.

## 7. Conclusions

Since pure nitrogen is the only effective atmosphere for aluminium sintering, it is obvious that the chemical reactions occurring between aluminium and nitrogen are of the greatest importance for the sintering process itself and for sintered properties. Initially, the protective aluminium oxide layer, being a sintering barrier, is disrupted thermally due to the CTE mismatch and structural transformation of alumina, which exposes the underlying metal and enables direct contact be-

tween aluminium and nitrogen. Further alumina disintegration may develop chemically, because creation of clean aluminium surfaces within the pores can allow nitrogen gas to react exothermally with aluminium to produce AlN, which results in self heating above the furnace temperature. Additionally, there are indications that nitrogen also goes into solution, which reduces the melting point at surfaces of powder particles that adjoin the pores. Because of its higher specific volume, the surface liquid will promote further disruption of any remaining oxide film and keep oxygen partial pressure low, allowing the nitrogen gas to further react with aluminium. Furthermore, the self-gettering mechanism and conversion of  $\gamma\text{-Al}_2\text{O}_3$  to AlN can contribute to disintegration of the alumina film.

To summarise, it may be concluded that the principal mechanisms of fracture and debonding behaviour of the alumina layer taking place during aluminium sintering in a nitrogen atmosphere are:

- thermal expansion mismatch,
- volume changes,
- liquid alloy formation and interfacial penetration,
- erosion through formation of volatile species.

## Acknowledgements

The research was supported by the grant POIG No. 01.01.02-00-015/09-00, which is gratefully acknowledged.

## REFERENCES

- [1] R.N. Lumley, T.B. Sercombe, G.B. Schaffer, *Metall. Mater. Trans. A*, **30A**, 457-463 (1999).
- [2] T. Pieczonka, Th. Schubert, S. Baunack, B. Kieback, *Mat. Sci. Eng. A*, **478**, 251-256 (2008).
- [3] T. Pieczonka, *Powder Metallurgy Processing of Aluminium*, in K. Świątkowski (Ed.) *Polish Metallurgy 2006-2010 in Time of the Worldwide Crisis* **1**, 37-57, Krynica (2010).
- [4] M. Ohring, *The Materials Science of Thin Films*, Academic Press Ltd, London, 1992.
- [5] W. Martienssen, H. Warlimont (Eds.), "Springer Handbook of Condensed Matter and Materials Data", Springer Berlin Heidelberg, 2005.
- [6] F. Fietzke, K. Goedicke, W. Hempel, *Surf. Coatings Techn.* **86-87**, 657-663 (1996).
- [7] G. Alcalá, P. Skeldon, G.E. Thompson, A.B. Mann, H. Habazaki, K. Shimizu, *Nanotechnology* **13**, 451-455 (2002).
- [8] S. Davis, G. Gutiérrez, *J. of Physics: Condensed Matter* **49**, 495401 (2011).
- [9] National Institute of Standards and Technology, *Ceramics Web-Book, Structural Ceramics Database (SCD)*, <http://www.ceramics.nist.gov/srd/scd/Z00291.htm>. 11.2012.
- [10] S.P. Adiga, P. Zapol, L.A. Curtiss, *Phys. Rev. B* **74**, 064204 (2006).
- [11] H. Momida, T. Hamada, Y. Takagi, *Phys. Rev. B* **73**, 054108 (2006).

- [12] R. Lizarraga, E. Holmström, S.C. Parker, C. Arrouvel, *Phys. Rev. B* **83**, 094201, (2011).
- [13] P.H. Poole, T. Granda, F. Sciortinod, H.E. Stanley, C.A. Angel, *Comp. Mat. Sci.* **4**, 373-382 (1995).
- [14] J.F. Shackelford, W. Alexander (*Eds.*), "CRC Materials Science and Engineering Handbook", CRC Press LLC, (2001).
- [15] S. Hasani, M. Panjepour, M. Shamanian, *Open Access Scientific Reports* **1**, 8, (2012), <http://www.omicsonline.org/scientific-reports/JMSE-SR-385.pdf>, 01.2013.
- [16] Website: TU Wien, Vapour Pressure Calculator, [http://www.iap.tuwien.ac.at/www/surface/vapor\\_pressure](http://www.iap.tuwien.ac.at/www/surface/vapor_pressure). 10.2013.
- [17] R. Sunderesan, P. Ramakrishnan, *Int. J. Powder Met. & Powder Techn.*, **14**, 9-16, (1978).
- [18] W. Kehl, H.F. Fischmeister, *Powder Met.* **23**, 113-119, (1980).
- [19] G.B. Schaffer, T.B. Sercombe, R.N. Lumley, *Mat. Chem. Phys.*, **67**, 85-91, (2001).
- [20] G.B. Schaffer, B.J. Hall, *Metall. Mat. Trans. A*, **33A**, 3279-3284, (2002).
- [21] T. Pieczonka, T. Schubert, S. Baunack, B. Kieback, *Proc. Conf. 'Sintering'05*, Grenoble 331-334, (2005).
- [22] T. Pieczonka, J. Kazior, M. Hebda, *Proc. World Congress & Exh. on Powder Metallurgy, Florence* **4**, 63-70 (2010).
- [23] T. Pieczonka, J. Kazior, M. Hebda, *PM<sup>2</sup>TEC 2011, Advances in Powder Metallurgy & Particulate Materials, San Francisco, MPIF* **5**, 20-30 (2011).
- [24] T. Pieczonka, J. Kazior, M. Nykiel, M. Hebda, *PM<sup>2</sup>TEC 2012, Advances in Powder Metallurgy & Particulate Materials, Nashville, MPIF* **5**, 1-9 (2012).
- [25] T. Pieczonka, J. Kazior, *Advanced Materials Research* **811**, 64-71 (2013).
- [26] Z.Q. Yang, L.Li He, S.J. Zhao, H.Q. Ye, *J. Phys.: Condens. Matter*, **14**, 1887-1893, (2002)
- [27] Z. Romanowski, S. Krukowski, I. Grzegory, S. Porowski, *J. Chem. Physics*, **114**, 6353-6363, (2001).
- [28] H.A. Wriedt, in T.B. Massalski (*Ed.*), *Binary Alloys Phase Diagrams*, ASM, Metals Park, OH, 1990.
- [29] H.L. Lukas, COST507 in Ansara (*Ed.*) *Thermochemical Database for Light Metal Alloys*, European Commission, 41 (1995).
- [30] *Calculated Al-N phase diagram*, National Physical Laboratory, (2010).
- [31] M. Hillert, S. Jonsson, *Metall. Trans. A* **23A**, 3141-3149 (1992).
- [32] Y. Du, R. Wenzel, R. Schmid-Fetzer, *Calphad*, **22**, 43-58 (1998).
- [33] T. Pieczonka, S.C. Mitchell, A.S. Wronski, J. Kazior, M. Hebda, *PM<sup>2</sup>TEC 2008, Advances in Powder Metallurgy & Particulate Materials, Washington, MPIF* **5**, 25-40 (2008).
- [34] J.H. Edgar, "Properties of Group III Nitrides", IET, (1994).
- [35] *Aluminum Nitride Material Properties*, leaflet, ACCURATUS Ceramic Corporation, <http://www accuratus.com>, 02.2013.
- [36] J.W. McCauley, "Structure and Properties of Aluminum Nitride and AlON Ceramics", Army Research Laboratory, Aberdeen Proving Ground, MD 210053069, (2002), <http://www.arl.army.mil/arlreports/2002/ARL-TR-2740.pdf>. 01.2013.
- [37] J.-M. Wagner, F. Bechstedt, *Phys. Rev. B* **66**, 115202, (2002).
- [38] J. Cheng, D. Agrawal, Y. Zhang, R. Roy, *J. Mat. Sci. Letters* **20**, 77-7, (2001).